Supplemental Information

# Cerebellar Control of Reach Kinematics

for Endpoint Precision

Matthew I. Becker and Abigail L. Person
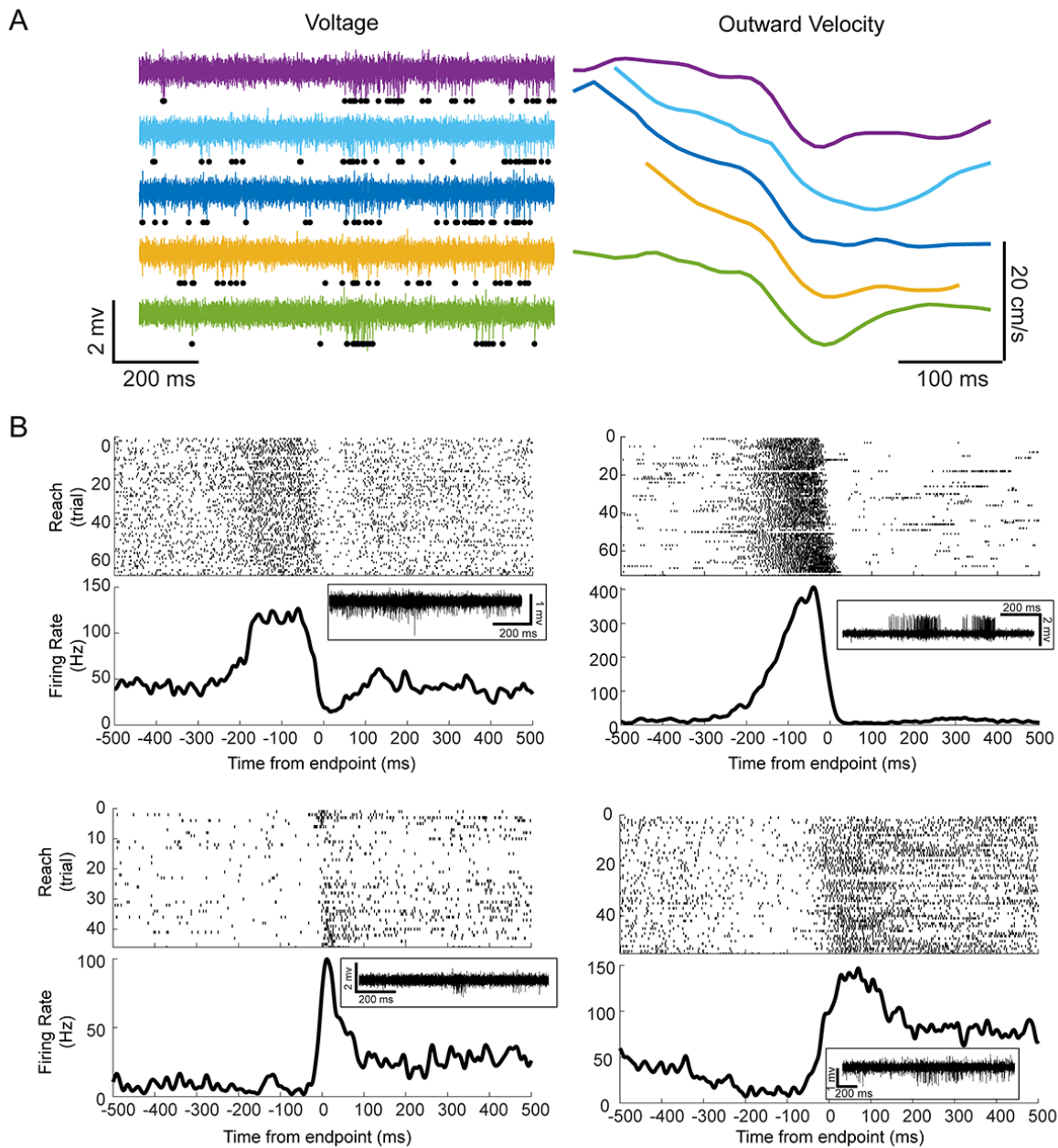
Figure S1. Related to Figure 1. Extracellular recordings of IntA neurons.
A. Example extracellularly-recorded voltage traces from a single tetrode lead on individual reach trials across a recording session (left; traces are aligned and centered on reach endpoint). Detected spikes are indicated by black dots. Corresponding single reach velocity profiles in the outward direction (right).
B. Four additional example rasters (top) and peri-event time histograms (bottom) of neurons recorded from IntA, aligned to reach endpoint. Insets display raw voltage traces high-pass filtered (250 Hz) for each neuron.
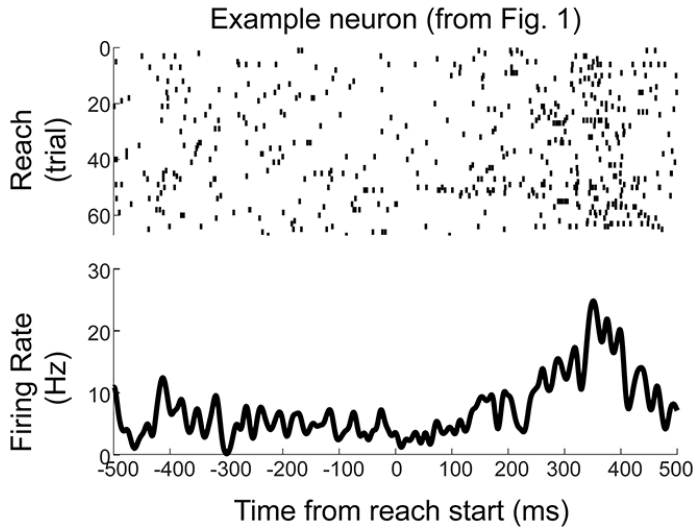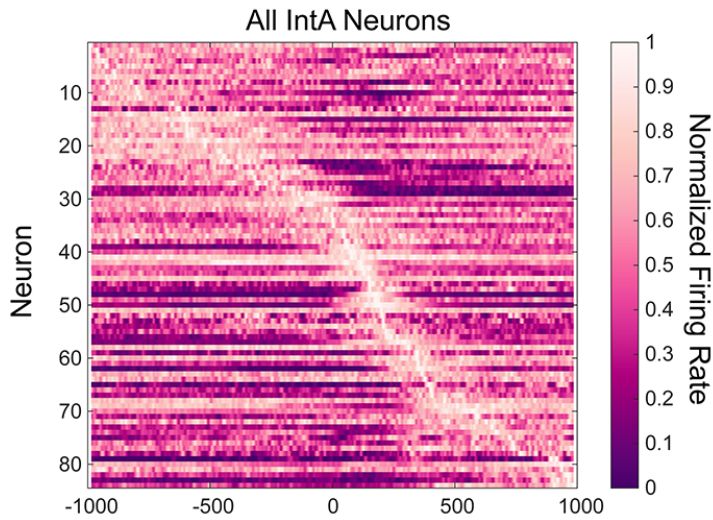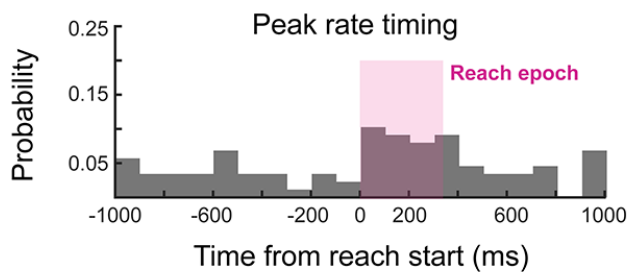
Figure S2. Related to Figure 1. IntA population activity aligned to reach start.
A. Raster (top) and PETH (bottom) of an example IntA neuron (same neuron as Figure 1B) aligned to reach start.
B. Population PETH including all cells recorded in IntA (n = 84) aligned to reach start and sorted by time of maximum firing rate (top). Firing rate is normalized to maximum on a per-cell basis. The reach epoch is highlighted in magenta (from reach start to average outreach duration of 313 ms).
C. Histogram of the timing of peak firing rates relative to reach start for all cells.
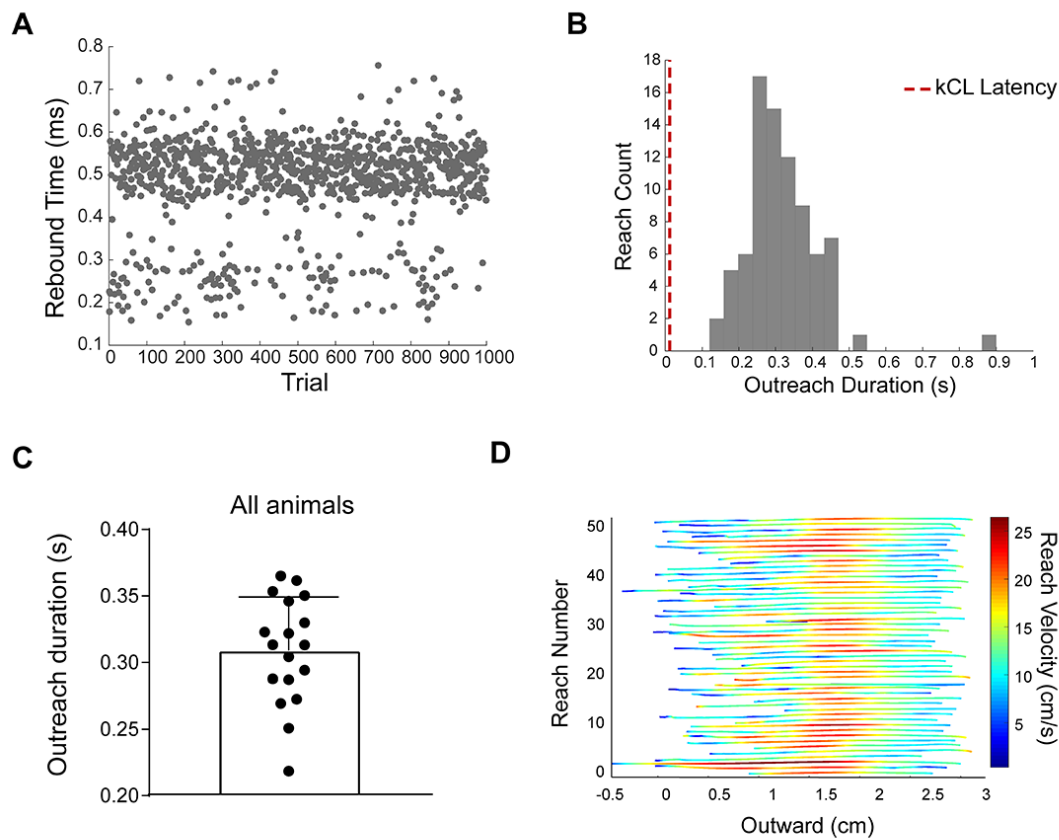
Figure S3. Related to Figure 2. Kinematic closed-loop system enables short-latency optogenetic stimulation at a precise kinematic landmark.

A. Performance latency of closed-loop reflection test between Matlab and Arduino for short latency communication.

B. Histogram of outreach duration for a single behavioral session (n = 82 reaches) compared to total latency of kinematic closed-loop stimulation system (9.5 ms).

C. Mean outreach duration for each animal (n = 18; black dots) and grand mean across the population of animals (bar).

D. Reach velocity (colorbar) as a function of outward position during 50 reaches from a single behavioral session. The consistent location of maximum outward velocity was chosen as the main kinematic landmark (1.6 cm from origin).
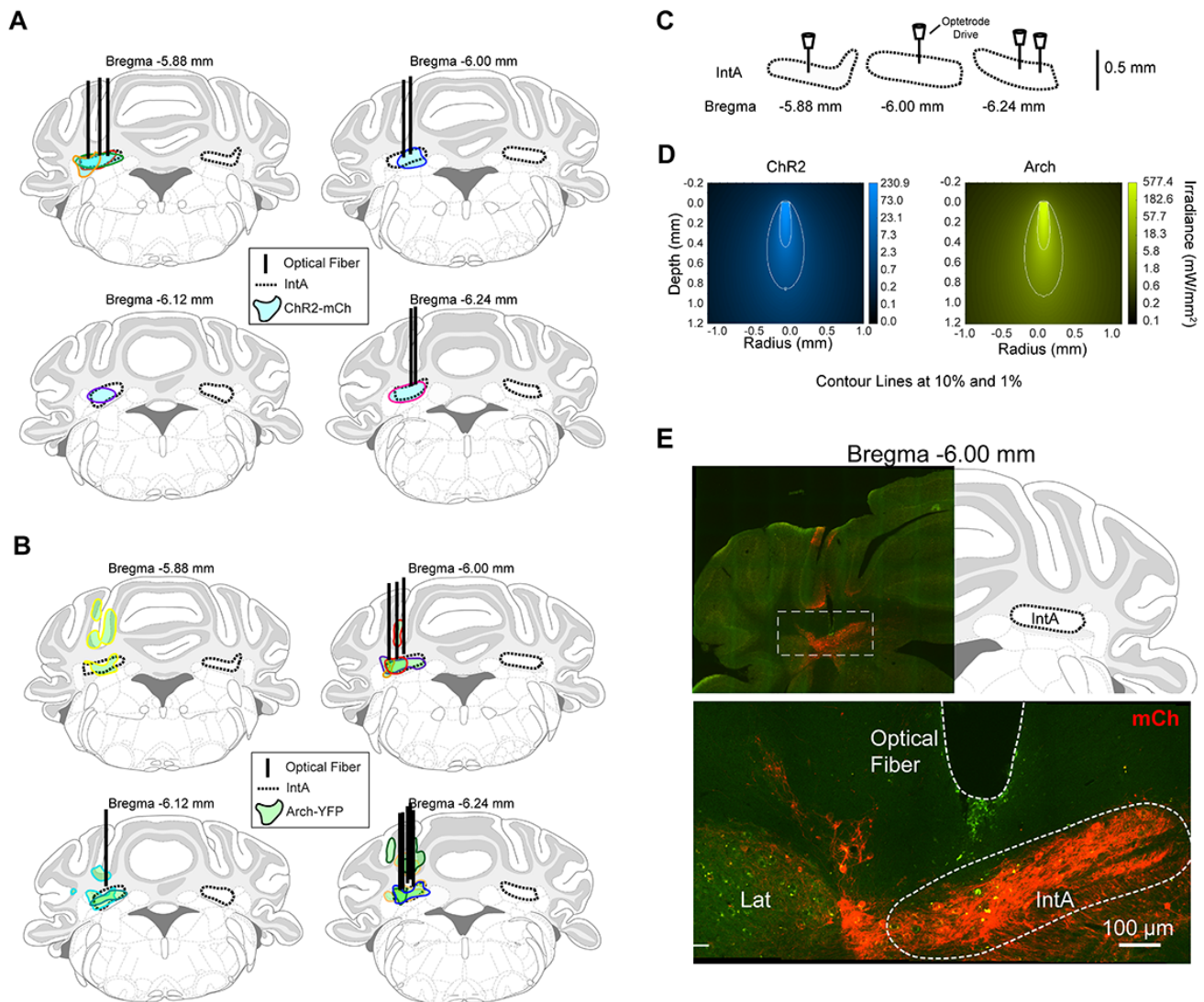
Figure S4. Related to Figures 2 through 7. Histological analysis of injection location, optical fiber placement, and drive placement in IntA.

A. Location of expression determined with confocal microscopy (contours) and fiber placement (black lines) in IntA for ChR2 animals. The contour for expression is displayed in a unique color for each animal.

B. Same as in **A** for experiments in which Arch is expressed.

C. Optetrode drive placements in IntA determined from post-hoc histological analysis.

D. Light spread analysis for highest optical power used in ChR2 experiments (2.0 mW; left) and Arch experiments (5.0 mW; rights). Contours illustrating 10% and 1% of maximum irradiance are indicated by white lines. Light spread falls off to 10% within 0.5 mm from fiber tip.

E. Example histological section. The specimen with the most off-target expression in the cerebellar cortex is displayed; no expression was noted in Purkinje neurons. Inset: mCh expression is largely confined to IntA, and optical fiber tip extends to just above the nucleus.
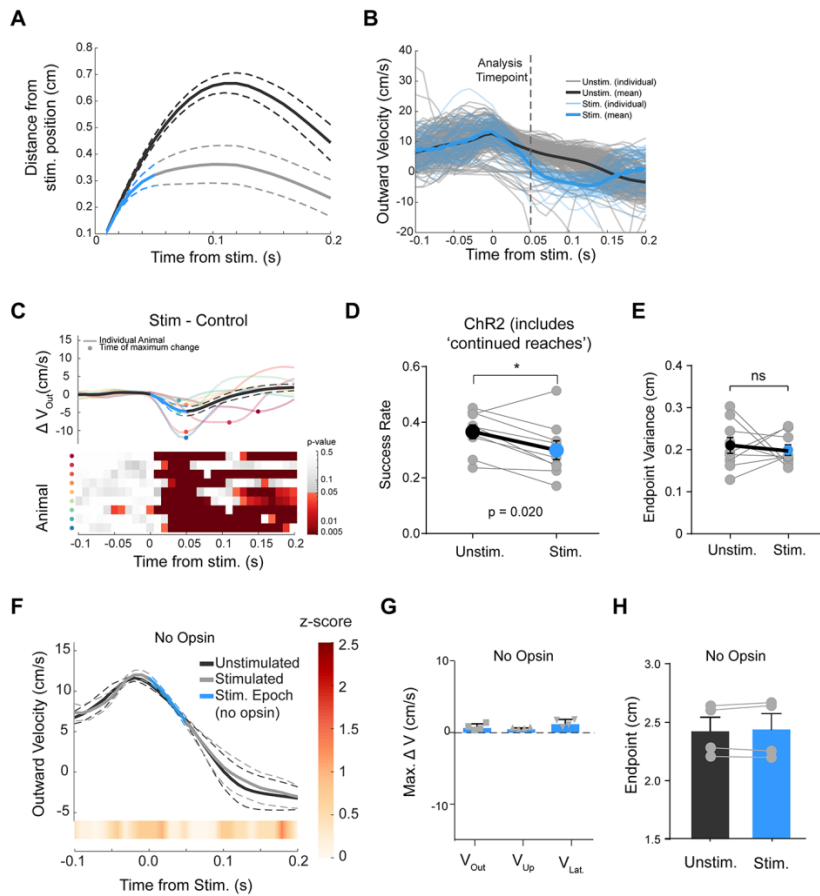
Figure S5. Related to Figure 2. Extended analyses of IntA excitation results and control experiments.
A. Average distance travelled over time following the stimulation trigger location for both stimulated (grey) and unstimulated reaches (black). Time of stimulation is indicated in blue.
B. Outward velocity over time for all unstimulated and stimulated individual reaches for a single animal (same data as Figure 2F).
C. Difference (Stim. – Unstim.) of velocity profiles for the population average (black) and all individual animals (colors). Heatmap of p-values associated with Wilcoxon rank sum tests conducted for each animal (rows) at 10 ms intervals (columns). Same data as Figure 2H.
**D.** Average success rates for each animal (grey dots) and the group mean (large black and blue dots) for IntA excitation with ChR2, compared to unstimulated reaches (paired t-test, p = 0.02). These data are for stimulation at the standard kinematic location and optical power only. Note that this definition of success rate included successful pellet retrieval on 'continued reaches' (see Figure 2C).
E. Average endpoint variance (standard deviation) for each animal (grey dots) and the group mean (large black and blue dots) for IntA excitation with ChR2, compared to unstimulated reaches (paired t-test, p = 0.67).
F. Population average of average outward velocity of unstimulated and stimulated reaches aligned to time of stimulation for mice with no opsin expressed in IntA (N = 4 animals). Blue indicates the stimulation epoch (50 ms, 2 ms pulses, 100 Hz). No significant difference was noted at any timepoint (p > 0.05) for any individual animal or for the population mean (N = 4 animals).
**G.** Summary of average maximum velocity effect magnitudes of stimulation in each of the three spatial dimensions across subjects (grey dots) and as a whole (bars) for 'no opsin' animals (Wilcoxon signed-rank, p = 0.13).
H. Average initial endpoint of unstimulated and stimulated reaches for 'no opsin' animals (paired t-test; p = 0.97).

5
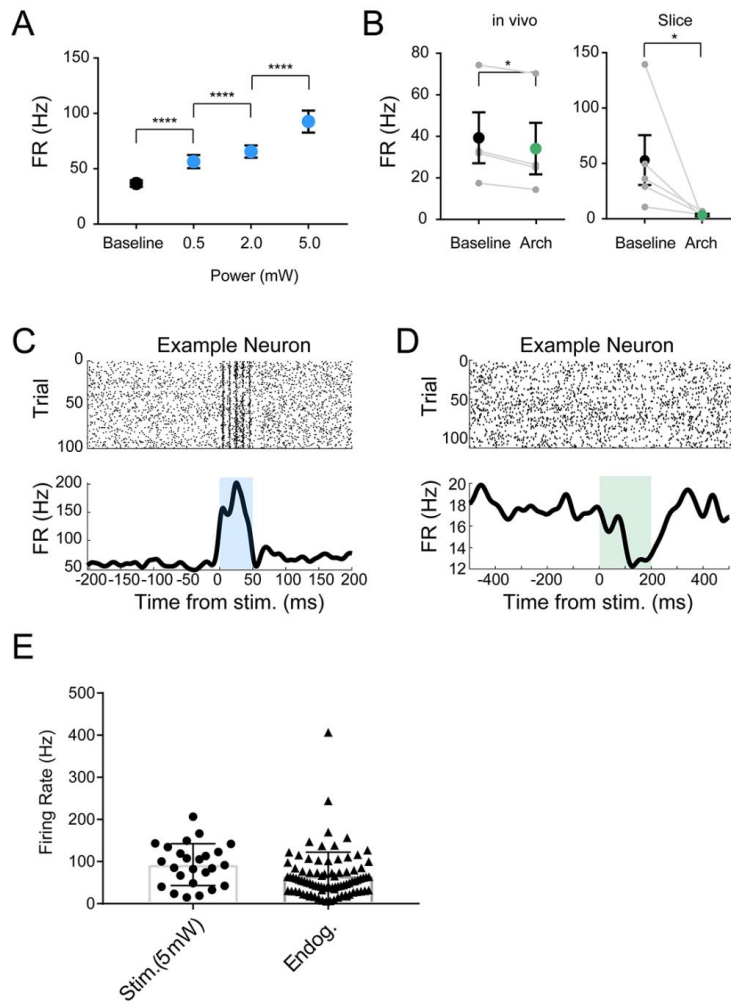
Figure S6. Related to Figure 3 and Figure 7. Recordings of IntA neurons during optogenetic stimulation.

A. Average firing rate of IntA neurons (n = 59) during baseline and ChR2 stimulation epochs at varying optical powers (**** p < 0.0001).

B. Average firing rate of IntA neurons recorded in vivo (left; individual neurons, grey; mean, black/green) and in slice (right) in response to Arch stimulation (in vivo: n = 4, * p = 0.012; in slice: n = 5, * p = .049).

C. Example raster and PSTH of ChR2-expressing neuron in response to 470 nm light stimulation (2.0 mW) using standard parameters used in this study (100 Hz, 2 ms pulses, 50 ms train).

D. Example raster and PSTH of Arch-expressing neuron in response to 561 nm light stimulation (5.0 mW) recorded in vivo.

E. Comparison of the distribution of firing rates under the strongest optical power tested (5.0 mW) with peak endogenous firing rates recorded during reach ('Endog.'). Similar ranges of firing rates were observed in these conditions.
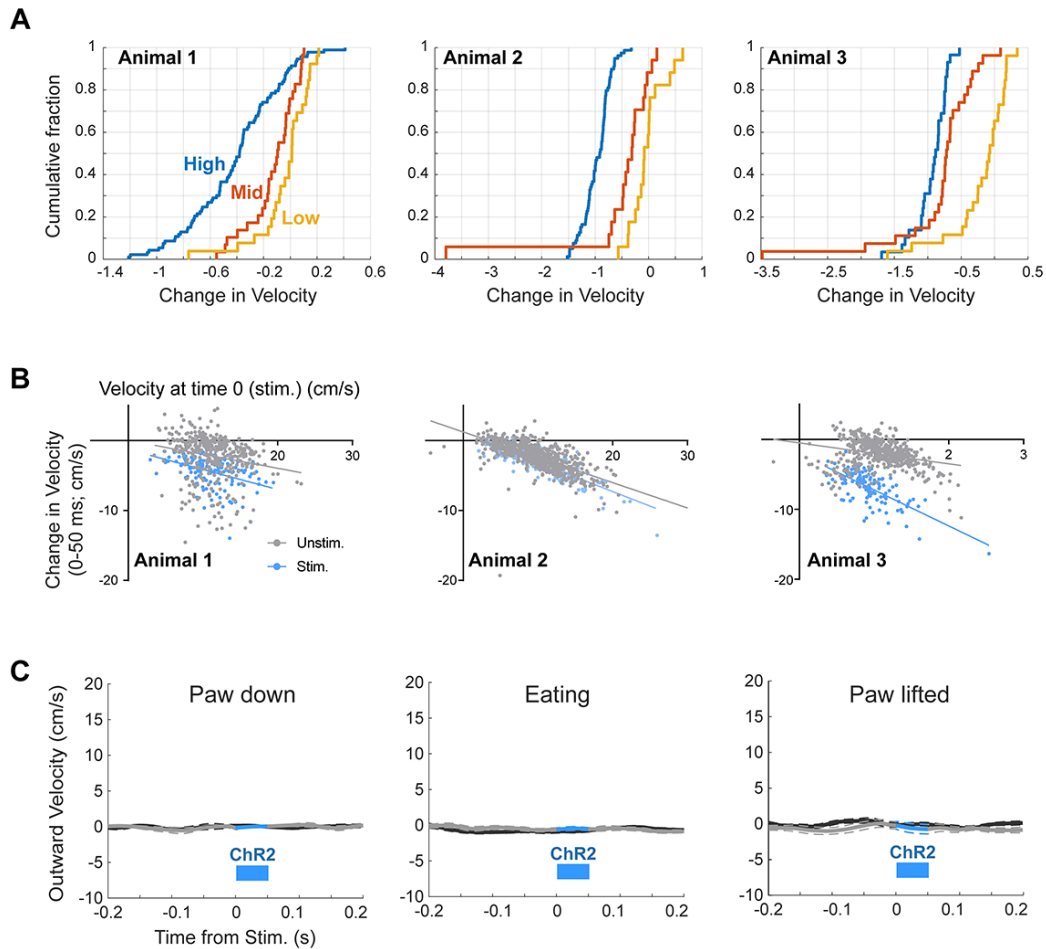
Figure S7. Related to Figures 3, 4, and 6. Extended kinematic analyses of various IntA stimulation conditions.

A. Distributions of velocity difference values (Stim. – Unstim.) at a specific latency for each of three optical powers (High, Middle, Low) for each animal tested. Within each animal, distributions were significantly different (Kolmogorov-Smirnov, $p < 0.05$), and means were significantly different (Wilcoxon rank sum, $p < 0.05$) across all pairs of neighboring conditions. Same data as Figure 3.

B. Relationship between outward velocity at the time of stimulation (time 0, x-axis) and subsequent change in velocity over the next 50 ms (y-axis) for unstimulated (grey) and stimulated (blue) reaches. All reaches that were recorded across different stimulation locations are plotted (Early, Middle, Late; same data as Figure 4). For Animals 1 and 2, regression lines had statistically indistinguishable slopes between unstimulated and stimulated reaches ($p > 0.05$), but significantly different y-intercepts ($p < 0.0001$), while the slope of the relationship decreased significantly for stimulated reaches in Animal 3 ($p < 0.0001$).

C. Outward velocity aligned to the time of stimulation for stimulated (grey lines; stim. epoch in blue) and unstimulated epochs, outside the context of active reaching behavior (N = 2 animals; n = 138 trials). Unstimulated epochs were drawn randomly from the continuous tracking data. Paw states (paw down, eating, and paw lifted) are described in Methods. No significant differences were measured in any context. Same data as Figure 6B.
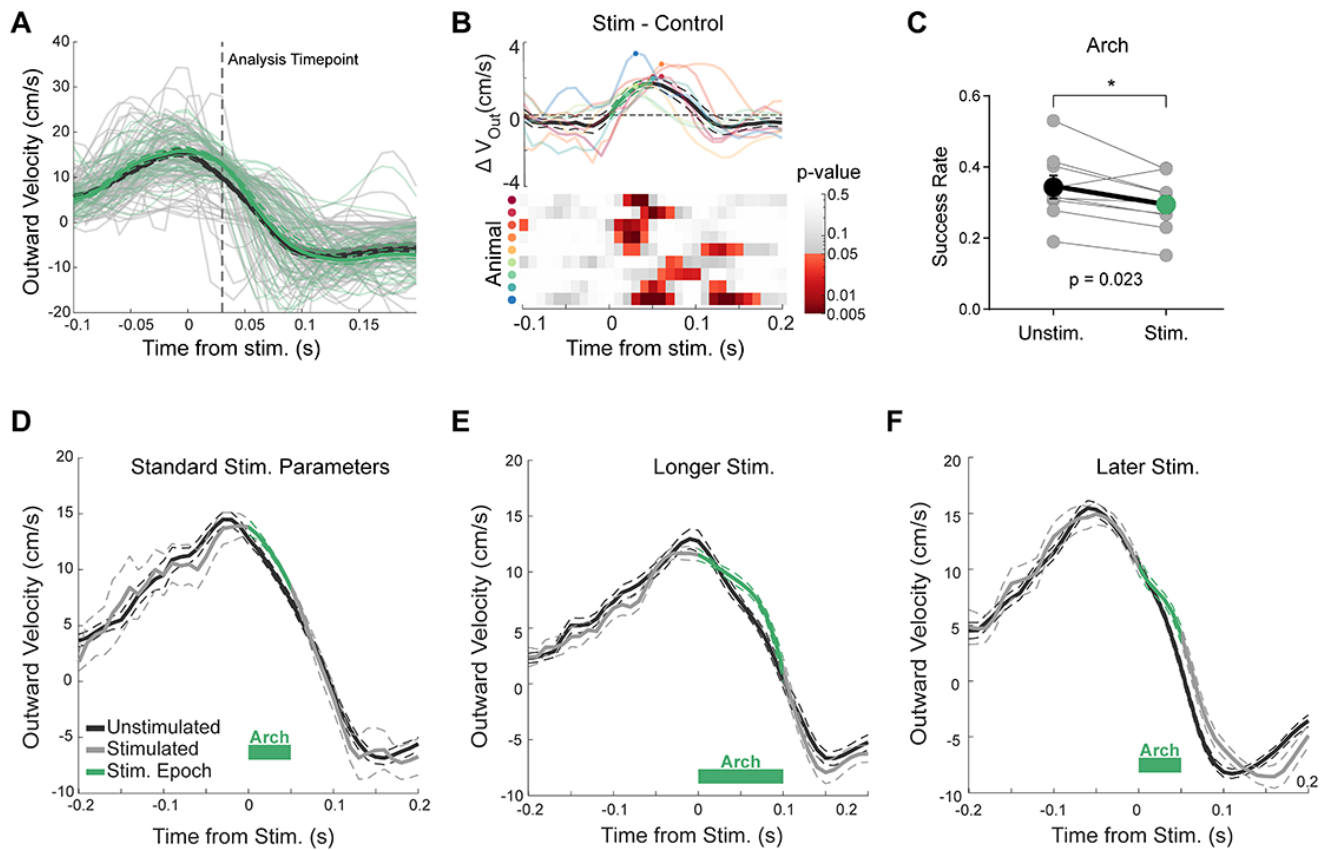
Figure S8. Related to Figure 7. Extended analyses and experiments for IntA inhibition

A. Outward velocity over time for all unstimulated and stimulated individual reaches for a single animal (same data as Figure 7A).

B. Difference (Stim. – Unstim.) of velocity profiles for the population average (black) and all individual animals (colors). Heatmap of p-values associated with Wilcoxon rank sum tests conducted for each animal (rows) at 10 ms intervals (columns). Same data as Figure 2H.

C. Average success rates for each animal (grey dots) and the group mean (large black and green dots) for IntA inhibition with Arch, compared to unstimulated reaches (paired t-test, p = 0.02).

D. Average outward velocity of unstimulated and stimulated reaches aligned to time of stimulation, using standard stimulation parameters (50 ms, standard kinematic landmark).

E. Representative example of average outward velocity of unstimulated and stimulated reaches aligned to time of stimulation (N = 3 animals), using longer duration stimulation (100 ms, standard kinematic landmark). Note that the magnitude of the effect is larger.

F. Representative example of average outward velocity of unstimulated and stimulated reaches aligned to time of stimulation (N = 2 animals), using the 'Late' kinematic landmark described in Figure 4 (50 ms, 'Late' kinematic landmark). Note that the location of the kinematic effect follows the location of stimulation.